Report #956541-Extension Final

REPORT ON

COMPENSATOR DEVELOPMENT AND EXAMINATION

OF PERFORMANCE AND ROBUSTNESS

6 March 1985

JPL CONTRACT NO. 956541

HR TEXTRON INC.

SYSTEMS ENGINEERING DIVISION
2485 McCabe Way
Irvine, California 92714

This work was performed for the Jet Propulsion Laboratory, California Institute of Technology. Sponsored by National Aeronautics and Space Administration under Contract NAS 7-918.

Report #956541-Extension Final

REPORT ON

COMPENSATOR DEVELOPMENT AND EXAMINATION

OF PERFORMANCE AND ROBUSTNESS

6 March 1985

JPL CONTRACT NO. 956541

HR TEXTRON INC.

SYSTEMS ENGINEERING DIVISION
2485 McCabe Way
Irvine, California 92714

This work was performed for the Jet Propulsion Laboratory, California Institute of Technology. Sponsored by National Aeronautics and Space Administration under Contract NAS 7-918.

ABSTRACT

This research focuses on the development of compensators to control the mean square surface error of a wrap-rib antenna. The approach is based on previous JPL sponsored research dealing with integrated control/structure design and modeling techniques for large space structures. The methodology is as follows: A model of appropriate size and structure is developed by looking at the convergence of functional gains for control and estimation. Then an LQG compensator is designed using this model. Finally, the compenstor is simplified using balanced realization thory.

In the conventional approach for compensator design, there is no mechanism for ensuring that the model is adequate for designing a compensator which will achieve the desired level of performance. It is shown here that both the model order and compensator order are directly related to the closed loop performance requirements for the system. The techniques developed in this report and in previous research provide a methodology for generating models and compensators of the required size.

The present report contains a number of simulations which describe the performance of the compensators developed here. For cases where the plant parameters are well known, excellent performance is obtained. The results, however, indicate the need for further work to improve robustness in the event that significant parameter errors are present.

TABLE OF CONTENTS

I. INTRODUCTION

I.1 Description of Project

This research has been an extension of the project discussed in the final report [1]. The main objective of both projects was to design a compensator based on a distributed model of a large flexible space antenna, and to compare this compensator to compensators based on purely finite dimensional models and methods. In both projects, linear quadratic optimal control and estimator theory and associated approximation theory were used to design the compensator. In the current project, the mean-square error of the reflecting surface is penalized directly in the performance index, whereas in the previous project, the total energy in the antenna was penalized in the performance index. Since the deflection of the reflecting surface is the main concern in controlling the antenna, penalizing this deflection explicitly should produce the best compensator. One advantage of distributed models is that they retain explicit physical descriptions of system components, like the mesh reflecting surface, thereby making it convenient to include the motion of certain components in a control performance index.

The compensator based on minimizing the mean-square surface error is presented in Chapter II and compared to a compensator based on minimizing the error of the antenna's rigid-body mode. Chapter III compares the performance of compensators designed using the approximation theory associated with distributed-system control theory to the performance of compensators designed using a conventional fixed-order finite

dimensional approach. The numerical results in Chapter III illustrate how the approximation methods developed in this and the preceding project guide the selection of the appropriate dimensions for the control model and compensator, and that these dimensions are functions of the performance requirements. The robustness of the compensator is discussed in Chapter IV.

I.2 Antenna Model and Finite Element Approximation

Description of Model

The space antenna model that has served as the primary example of this research is shown in Figure 1.1. The flat antenna consists of a rigid hub, eight ribs and a mesh reflecting surface. The ribs are modeled as beams cantilevered to the hub, and the mesh is modeled as circular sectors of membrane tied to the ribs and hub. The center of the hub is fixed but the hub can rotate out of plane, so that there are two rigid-body modes.

This model is based on the Lockheed wrap-rib antenna [2]. Since this is the first truly complex structure to which the methods of the current research have been applied, the model has been simplified to a flat antenna with eight instead of the actual 48 ribs, to allow concentration on fundamental issues while maintaining a complex structure with different types of components. Otherwise, the parameters given in Figure 1.1 are based on the 48-rib antenna [3].

The two actuators apply torques to the hub, and the sensors measure the rotation of the hub and the displacement of the tip of each rib relative to the hub plane. The compensator

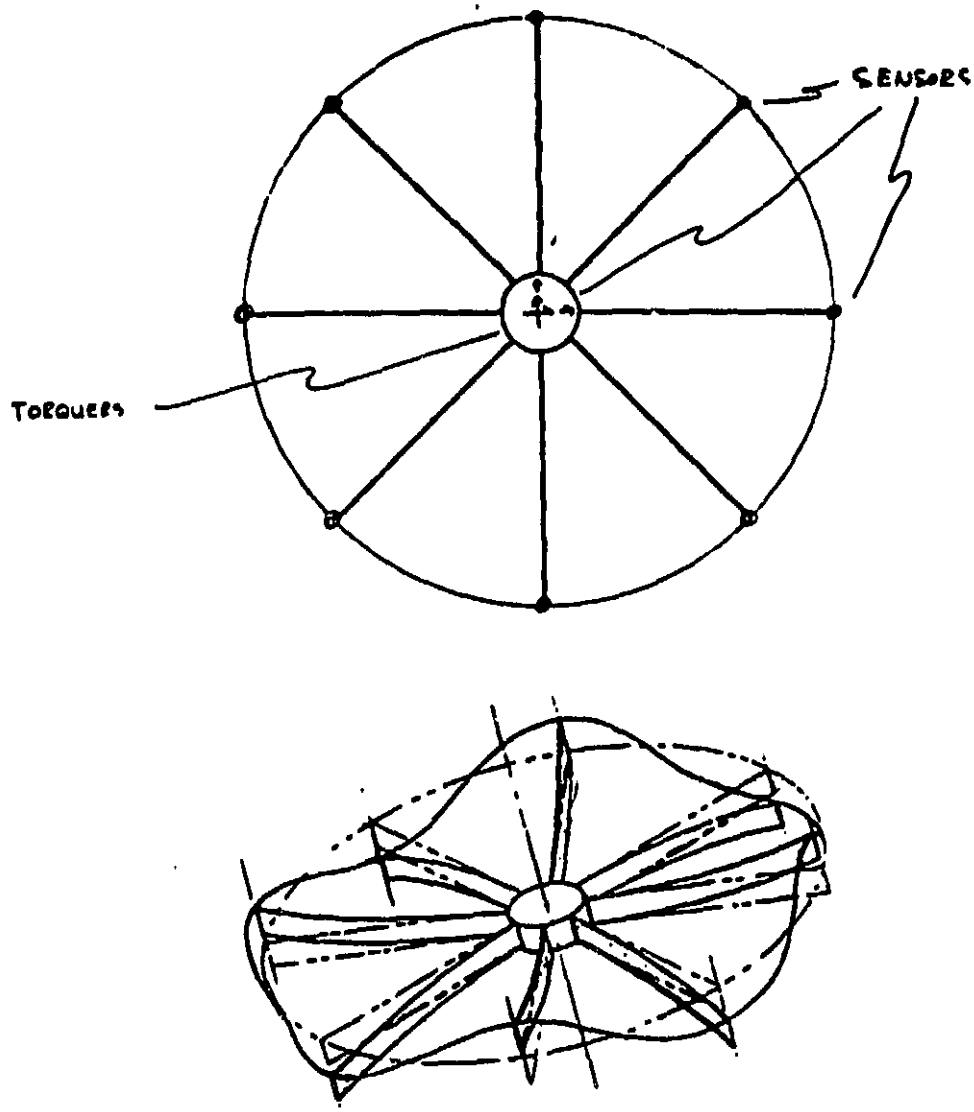

MODEL DATA (based on 48 rib Lockheed wrap rib antenna):

Hub Radius: 46 in. Hub Weight: 1000 lbs.

Hub Inertias: $I_{xx} = I_{yy} = 342$ lb-in-sec^2
$I_{zz} = 684$ lb-in-sec^2

Rib Length: 86 ft. Rib Weight: 115 lb. per rib

Rib stiffness: EI = 4.05×10^7 lb-in^2

Mesh Weight: 6.94 lb per sector

Space Antenna Model

Figure 1.1

is designed to control the linear out-of-plane motion of the antenna.

For small elastic displacements, the symmetry of the antenna further reduces the complexity of the compensator design because the motion of the antenna can be separated into two sets of orthogonal modes, with each set controlled independently by one actuator. Each of these sets of modes consists of those modes which are asymmetric about one of the torque axes. Modes symmetric about both torque axes are uncontrollable. Although the actuators can control only the controllable modes, these are the only modes that are excited by rotating the antenna with the torquers on the hub.

Viscoelastic damping is modeled in both ribs and mesh. If the stiffness operator A_o is separated into rib and mesh components as

$$A_o = A^r{}_o + A^m{}_o, \tag{1.1}$$

then the damping operator is

$$D_o = C^r A^r{}_o + C^m A^m{}_o \tag{1.2}$$

If $C^r \neq C^m$, this structural damping couples the natural modes but not modes which are controllable by a given actuator with modes which are uncontrollable by the same actuator.

Approximation of Antenna

The approximation scheme used in the control problem was a component modal synthesis for which the component modes of the ribs and mesh were determined by consistent-mass finite element approximations. For the mesh sectors, an explicit Galerkin approximation was used. For details on this

approximation scheme, see Chapter 2 of [1].

An important advantage of the finite element approximation used in this project is that it is easy to vary the order of approximation in the individual structural components. Because the performance required of the control system determines the accuracy of approximation necessary in designing a controller, it is impossible to know in advance what order of approximation will be required. The subsequent sections of this report illustrate the importance of an approximation scheme that allows the model order to be varied easily.

II. COMPENSATOR BASED ON MEAN-SQUARE SURFACE ERROR IN PERFORMANCE INDEX

II.1 COMPENSATOR DERIVATION

In this chapter, a compensator has been synthesized which minimizes the mean-square surface error of the antenna described in Chapter 2 of Ref. [1]. The compensator is based on the techniques documented in Ref. [1].

The performance index for the optimal control problem for the antenna has the form

$$J = \int_0^\infty (\langle Qz, z\rangle + r\, u^2),\ dt \qquad (2.1)$$

where z is the state vector and u is the control torque. For the compensator in this report, the operator Q was chosen so that $\langle Qz,z\rangle$ is

$$q_1\theta^2 + q_2\dot{\theta}^2 + q_3 \int_{A_{mesh}} W^2_{mesh}\ dA_{mesh} \qquad (2.2)$$

where θ is the rigid body angle and W_{mesh} is the displacement of the mesh reflecting surface from the position in which the rigid-body rotation and all elastic deformations are zero. It may be noted that the third term in this expression penalizes rigid body rotation as well as elastic deformation, so rigid body rotation appears in two terms of $\langle Qz,z\rangle$.

In choosing the weighting coefficients q_1, q_2, q_3 and r, we took the mean-square surface error weighted by q_3 as the

primary term to be minimized, but we also considered the response time and overshoot of the rigid-body angle to be secondary objectives. After considerable analysis and numerical experimentation with different sets of q_1, q_2, q_3 and r we selected

$$\text{(CASE 1)} \quad q_1 = 0., \; q_2 = 0., \; q_3 = 374., \; r = .0001.$$

The estimator used in the compensator is the same one used in the compensator described in Ref. [1].

Figures 2.1 and 2.2 show the Bode plots of the ideal compensator for Case 1. The compensator has three channels. Channel 1, shown in Figure 2.1, is from the hub rotation sensor to the torque actuator. Channels 2 and 3 are from each of the two rib tip displacement sensors to the torque actuator, and because of the antenna symmetry, these channels have identical transfer functions. The frequency response of Channel 2 (or 3) is shown in Figure 2.2. Figure 2.3 shows the response of the rigid-body angle, the mean square surface error

$$(\text{RMS})^2 = \int_{A_{\text{mesh}}} w^2_{\text{mesh}} \; dA_{\text{mesh}} \qquad (2.3)$$

and the control u(t) for the initial condition consisting of an initial rigid-body rotation only.

For comparison, we computed the compensator for (CASE 2) $q_1 = 74.$, $q_2 = 0.$, $q_3 = 0.$, $r = .0001$. If the antenna were rigid, CASE 1 and CASE 2 would be equivalent. The comparison then illustrates the difference, in the presence of flexible ribs and mesh, between penalizing the actual error of the reflecting

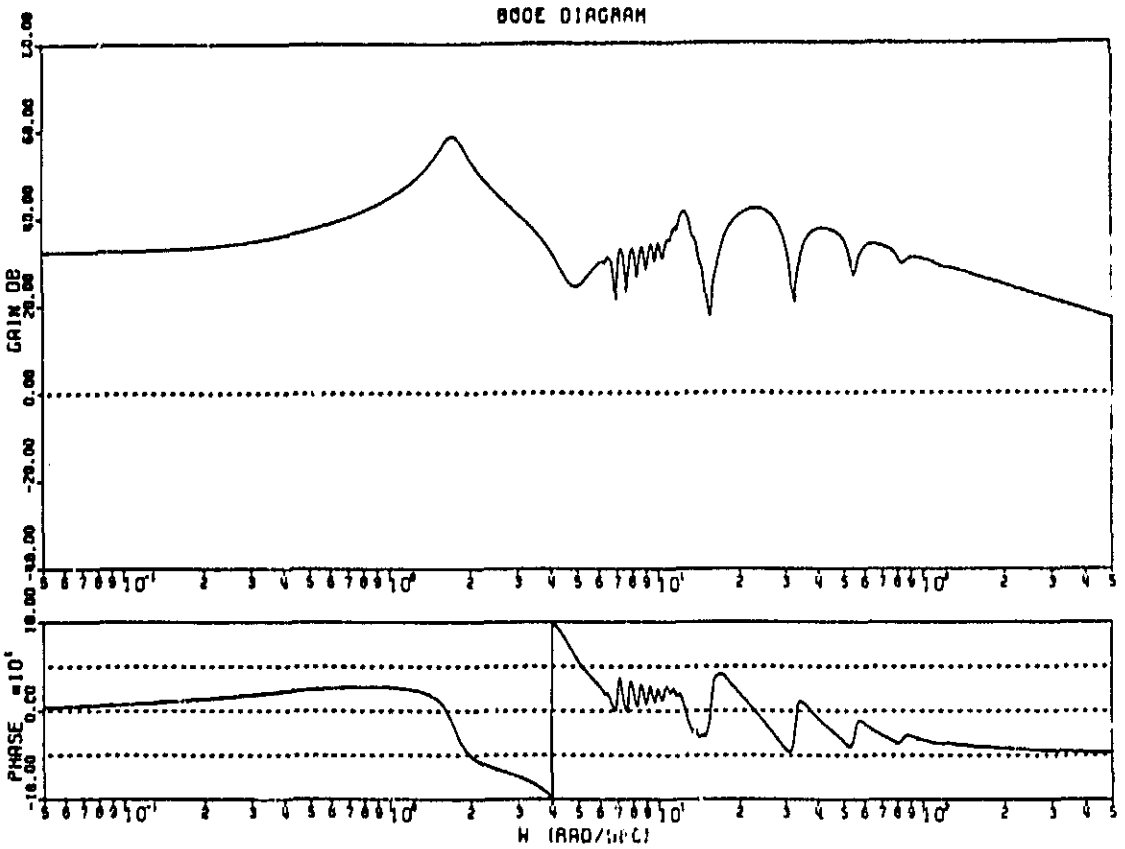

Figure 2.1

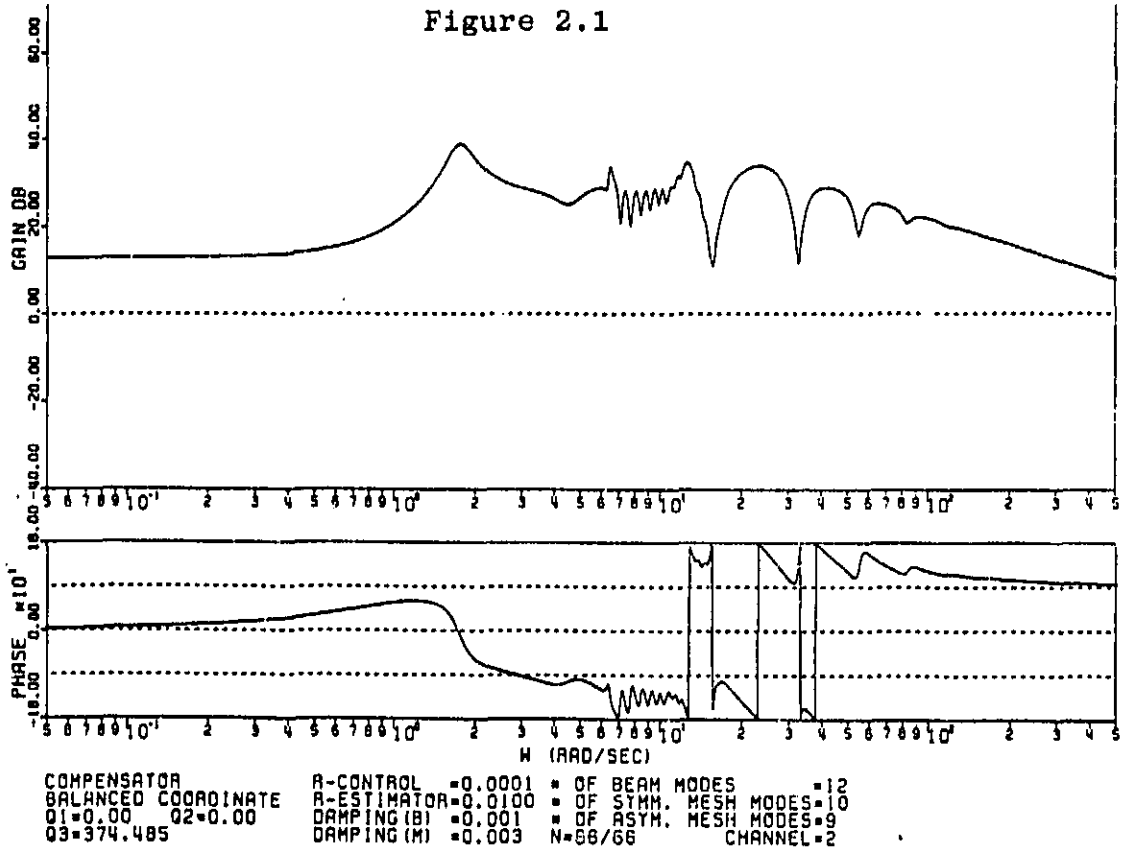

Figure 2.2

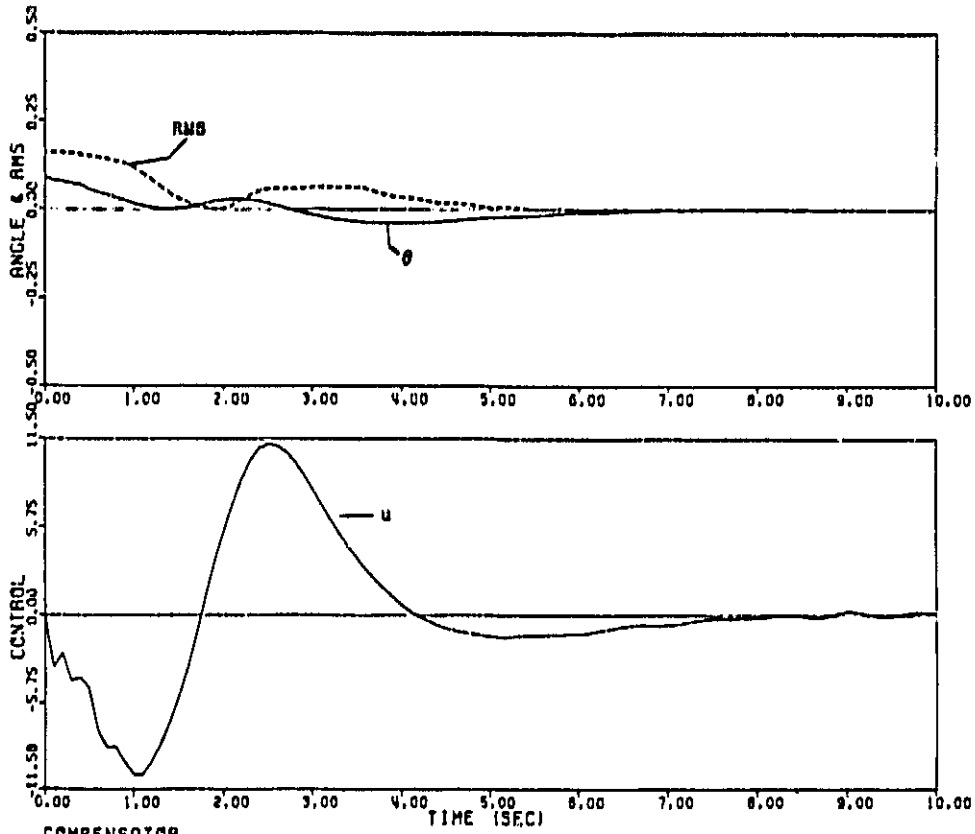

COMPENSATOR
Q1=0.00
Q2=0.00
Q3=374.485
IC=MODE=1

R-CONTROL =0.0001 # OF BEAM MODES =12
R-ESTIMATOR=0.0100 # OF SYMM. MESH MODES=10
DAMPING(B) =0.001 # OF ASYM. MESH MODES=3
DAMPING(M) =0.003 N=40/66

Figure 2.3

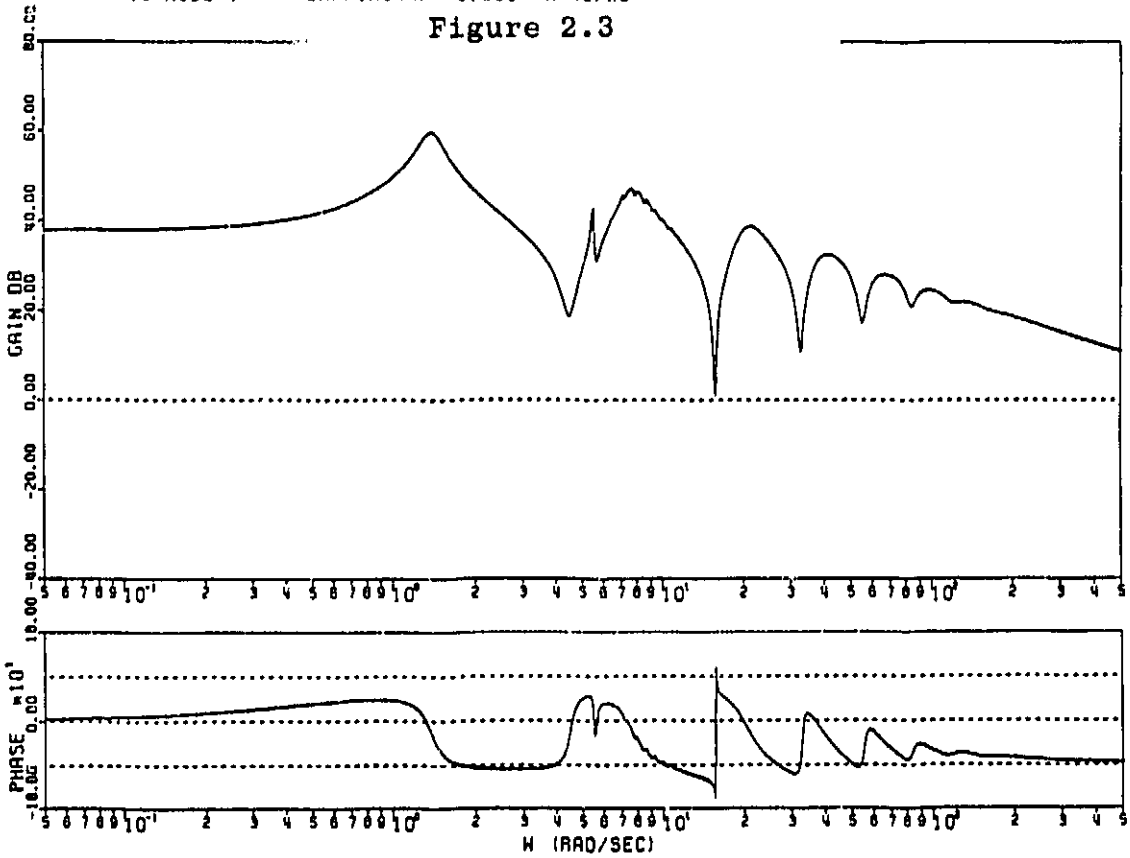

COMPENSATOR
BALANCED COORDINATE
Q1=73.53 Q2=0.00
Q3=0.00

R-CONTROL =0.0001 # OF BEAM MODES =12
R-ESTIMATOR=0.0100 # OF SYMM. MESH MODES=10
DAMPING(B) =0.001 # OF ASYM. MESH MODES=9
DAMPING(M) =0.003 N=66/66 CHANNEL=1

Figure 2.4

surface and penalizing just the rigid-body rotation. Figures 2.4 and 2.5 show the Bode plots for Channels 1 and 2 of the CASE 2 compensator, and Figure 2.6 shows the corresponding rigid-body angle, mean-square surface error and the control u(t) for the initial condition consisting of an initial rigid-body rotation only.

The Bode plots indicate that the compensator for CASE 1 takes the mesh modes into account significantly, while the compensator for Case 2 virtually ignores the mesh. Figures 2.3 and 2.6 appear to confirm this interpretation, since the compensator for CASE 1 produces significantly less mean-square surface error.

II.2 CONCLUSION

A compensator has been synthesized to minimize the mean-square error of the wrap-rib antenna. The numerical results show that including the flexible modes of the antenna in the performance criterion leads to better performance than basing this criterion on rigid body rotation only.

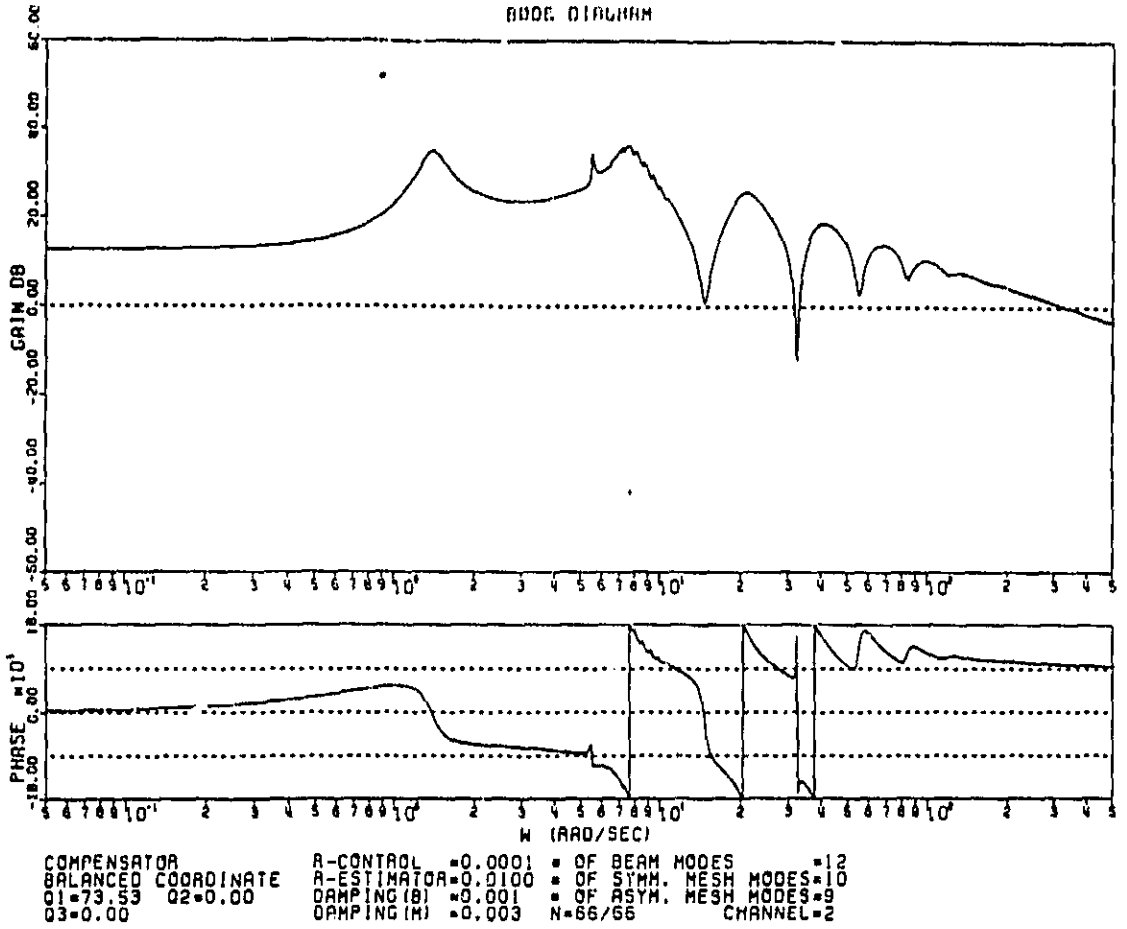

Figure 2.5

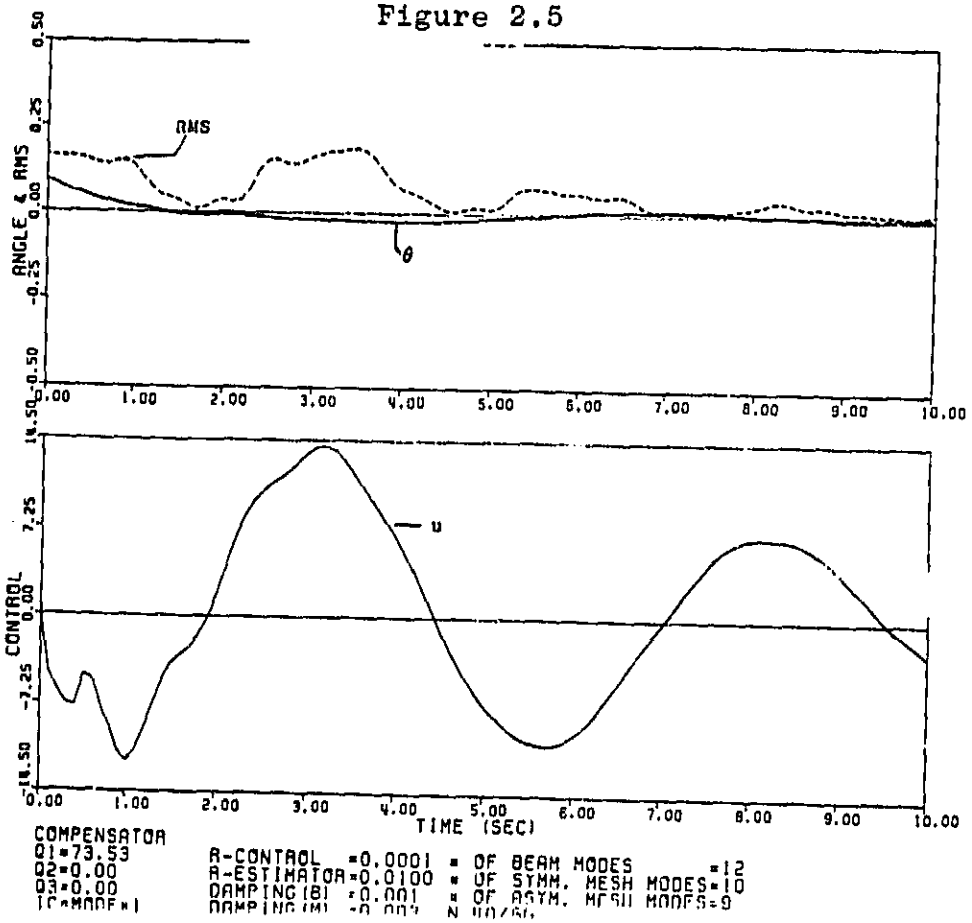

Figure 2.6

III. COMPARISON OF COMPENSATORS GENERATED BY CONVENTIONAL METHODS WITH COMPENSATORS GENERATED BY THE PRESENT APPROACH

III.1 INTRODUCTION

The compensator design procedure used in this research is one which integrates the process of modeling a physical system with that of designing a controller for the system. In the conventional approach, these two phases of control system design are performed independently. The following section compares the performance obtained from the conventional approach with that obtained from the integrated approach.

A common procedure for designing a compensator for a flexible structure is to choose a fixed order finite element model of the structure and then design the compensator for that model. The problem with this method is that it fails to recognize that the order of the model necessary for designing an effective compensator varies with the performance requirements and also the location and characteristics of the sensor and actuator hardware. For example, the faster the desired response, the larger the order of model necessary for designing a compensator to produce the desired response.

Both the stability of the closed loop system and the values of the closed loop performance indices will in general differ if the different procedures are used to design the controller. Our work under this contract is focused on generating quantitative measures which will allow us to evaluate

these differences for a conventional versus the integrated approach. Both numerical and graphical results are presented in the next section.

III.2 RESULTS

Comparison of conventional and integrated design procedures has been carried out with respect to a performance index which seeks to minimize the root mean square surface of space antenna described previously. This index is the same as that given in Equations (2.1) and (2.2) with q_1 and q_2 set equal to zero, q_3 set equal to ρ, and r set equal to 1. Repeating the index here for convenience we have

$$J = \int_0^\infty [\rho\ (RMS)^2 + u^2]\ dt \qquad (3.1)$$

making ρ larger indicates increased performance is desired. The cost function of Equation (3.1) contains two parts:

$$J_x = \int_0^\infty \rho (RMS)^2 dt; \quad J_u = \int_0^\infty u^2 dt \qquad (3.2)$$

J_x is the quantity we actually wish to control, and J_u is the cost of achieving this control.

To explore the relation between performance desired and model order required, we employed the following procedure:

1) Select a model consisting of N modes. (The model order will be 2N). The N modes are selected on the basis of internal balancing to insure that they are important for the input/output description of the model. (See [1]).

2) Select a value for ρ beginning with a small value, such as .001.

3) Design a compensator using standard LQG theory. The order of the compensator will be 2N.

4) Apply the compensator to a model which is sufficiently large to represent a highly accurate "truth" model of the system. The model we used contained 40 modes.

5) Compute the values of J_x and J_u which result when the 2N-th order compensator is applied to the truth model. This requires specification of a particular set of initial conditions. We assumed a rigid body rotation of the entire antenna.

6) Repeat steps 2) through 5) using a larger value of ρ .

7) For sufficiently large ρ, the model of order 2N will not produce a satisfactory compensator, and instability will be observed in step 5). When this happens, increase the value of N and start again at step 1).

The procedure outlined was performed for N = 6, 8, 12, 16 and 22 and values of ρ ranging from .001 to 1000. The results are displayed in Table 3.1 and Figures 3.1 and 3.2 The general trends are more easily seen using the figures.

Figure 3.1 shows that for ρ = .001 and .01 (low performance) all of the models are almost equally effective in producing an acceptable compensator. When ρ = .1, compensators

N \ ρ	0.001	0.01	0.1	1.0	10	100	1000
6	1.431*	0.955	0.820	UNSTABLE →			
8	1.422	0.934	0.810	0.864	UNSTABLE →		
11	1.416	0.919	0.808	0.851	0.858	UNSTABLE →	
16	1.418	0.914	0.723	0.680	0.670	0.668	UNSTABLE
22	NC**	NC	0.709	0.666	NC	NC	0.651

* NUMBERS IN TABLE ARE VALUES OF J_x FOR DIFFERENT VALUES OF N, ρ.

** NC = NOT COMPUTED

TABLE 3.1 PERFORMANCE COMPARISON

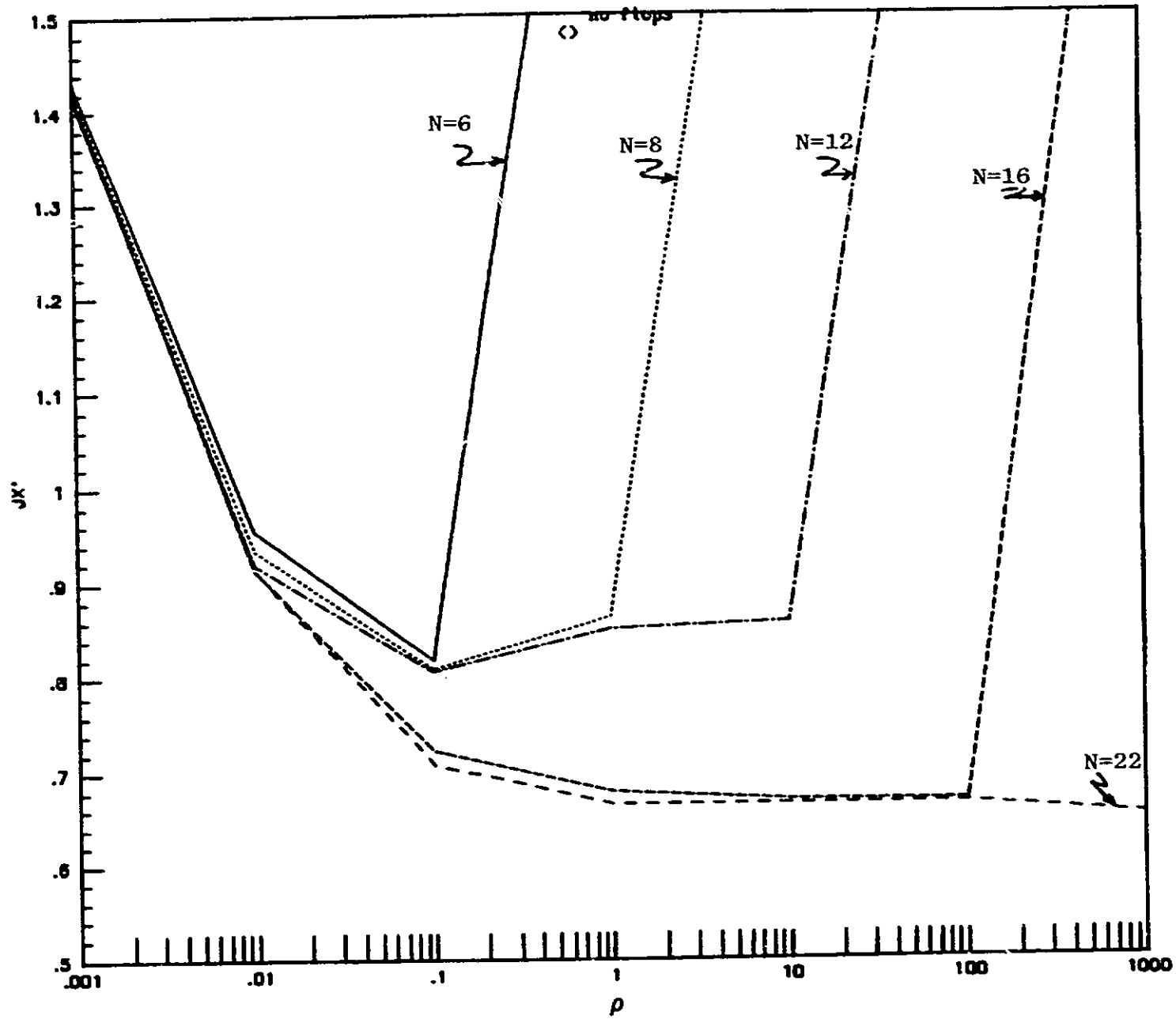

Figure 3.1

Performance of various compensators as a function of weighting factor ρ. The parameter is the N, the modes the compensator is based on.

LEGEND

⊠ J_x value for N=6

⊗ J_x value for N=8

□ J_x value for N=12

x J_x value for N=16

0 J_x value for N=22

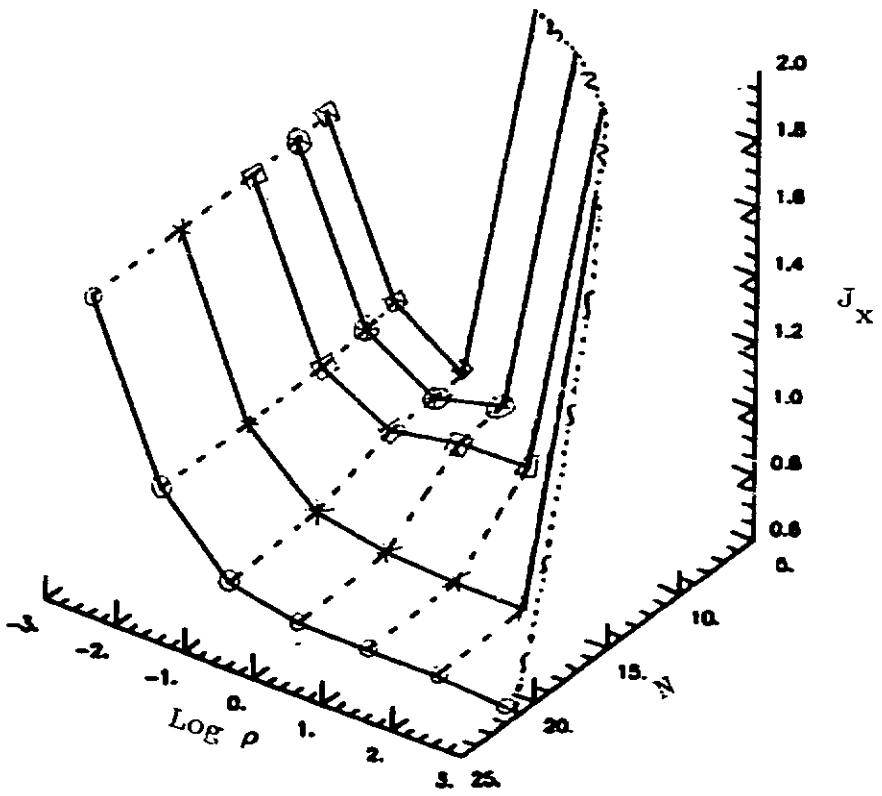

Figure 3.2

Performance of various compensators as a function of modes N and weighting factor ρ.

based on the higher order models (N=16,22) begin to show superior performance compared to those based on the lower order models. At ρ = 1.0, the compensator based on the 6 mode model has destabilized the system, and that based on the 8 mode model is on the verge of doing so. As ρ is increased further, compensators based on 8, 16, and 22 mode models each in turn destabilize the system.

The information displayed in Figure 3.2 is essentially the same as that displayed in Figure 3.1, except it is presented in a three dimensional format. This figure is particularly suited for seeing the relationship between the conventional LQG compensator design procedure, and that developed in this research. In the conventional approach, there are no guidelines for selecting a model whose order is appropriate for the control problem at hand. Without such guidelines, one might select an unnecessarily large model resulting in a complicated compensator with no significant improvement in performance. (Consider that for ρ= 0.001, the compensator based on N=6 performs as well as that based on N=22.) On the other hand, one might select a model which is too small leading to severely degraded performance or even instability. (Consider ρ= 10 and compare the performance of the compensators based on N=8 and 16.) By looking at the convergence of the functional gains and of the frequency response (see [1]), the approach employed in this research directly considers how many modes and which modes need to be included in the model, and thus insures that the model is of the right size and contains the right modes. When the appropriate model is used

to design the compensator, one has some confidence that the compensator obtained will not change significantly if more modes are used. In this case, the compensator may be said to have "converged."

After a converged compensator is obtained, further simplification may still be possible. For example, near pole-zero cancellations may be eliminated without significant loss of performance. Minor features of the compensator may also be relatively unimportant in the high frequency range where the compensator strongly attenuates any incoming signal. Direct compensator simplification (as opposed to plant model reduction) can be accomplished through the use of balanced realizations. This method identifies compensator dynamics which do not contribute strongly to the overall compensator frequency response. This technique has been successfully applied to the compensators described in Reference 1 and in Chapter II of the present report.

Figures 3.3 through 3.11 contain a number of time histories which amplify and confirm the information contained in Figures 3.1 and 3.2. The upper graph of each figure shows the hub angle (solid line) and RMS surface error (dashed line) as a function of time. The bottom graph shows the hub torque as a function of time. In each case, the initial condition is a rigid body rotation of the entire antenna, and the objective is to bring the antenna back to zero. The motion is essentially a slew maneuver.

Figures 3.3 and 3.4 are for N=6 and for ρ =.01 and .1. Although the character of the two plots is similar, the plot for

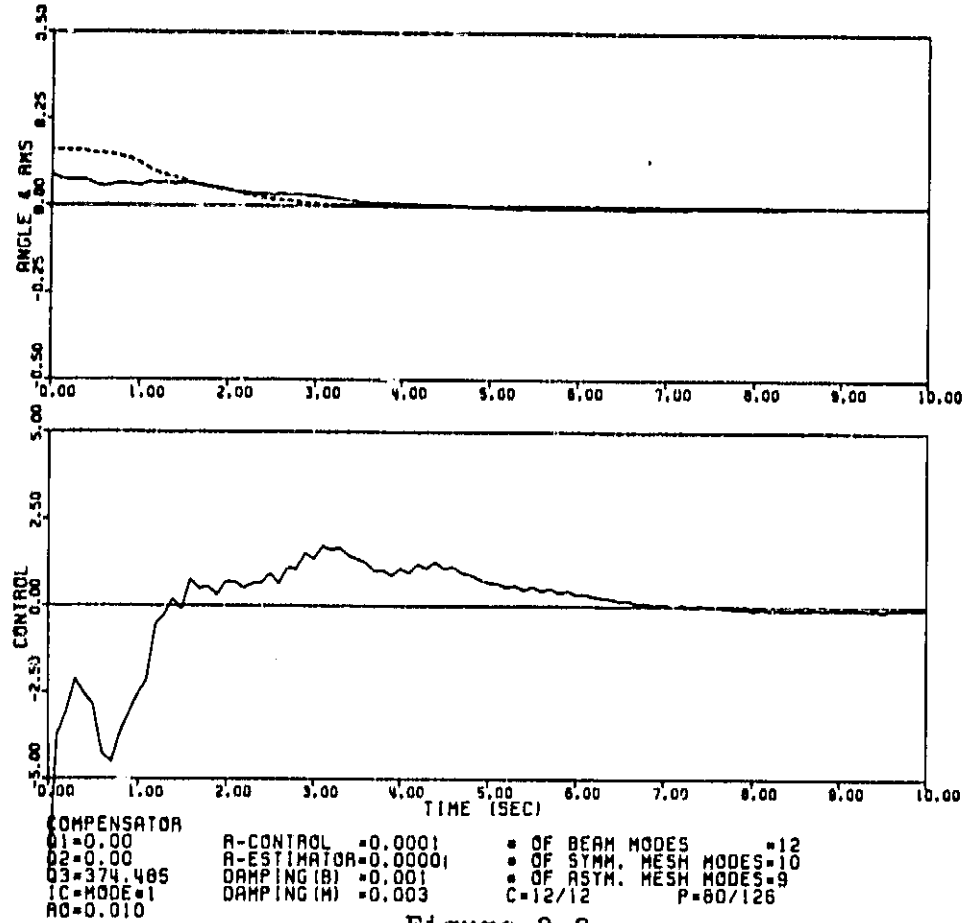

COMPENSATOR
Q1=0.00
Q2=0.00
Q3=374.485
IC=MODE=1
R0=0.010

R-CONTROL =0.0001
R-ESTIMATOR=0.00001
DAMPING(B) =0.001
DAMPING(M) =0.003

# OF BEAM MODES =12
# OF SYMM. MESH MODES=10
# OF ASYM. MESH MODES=9
C=12/12 P=80/126

Figure 3.3

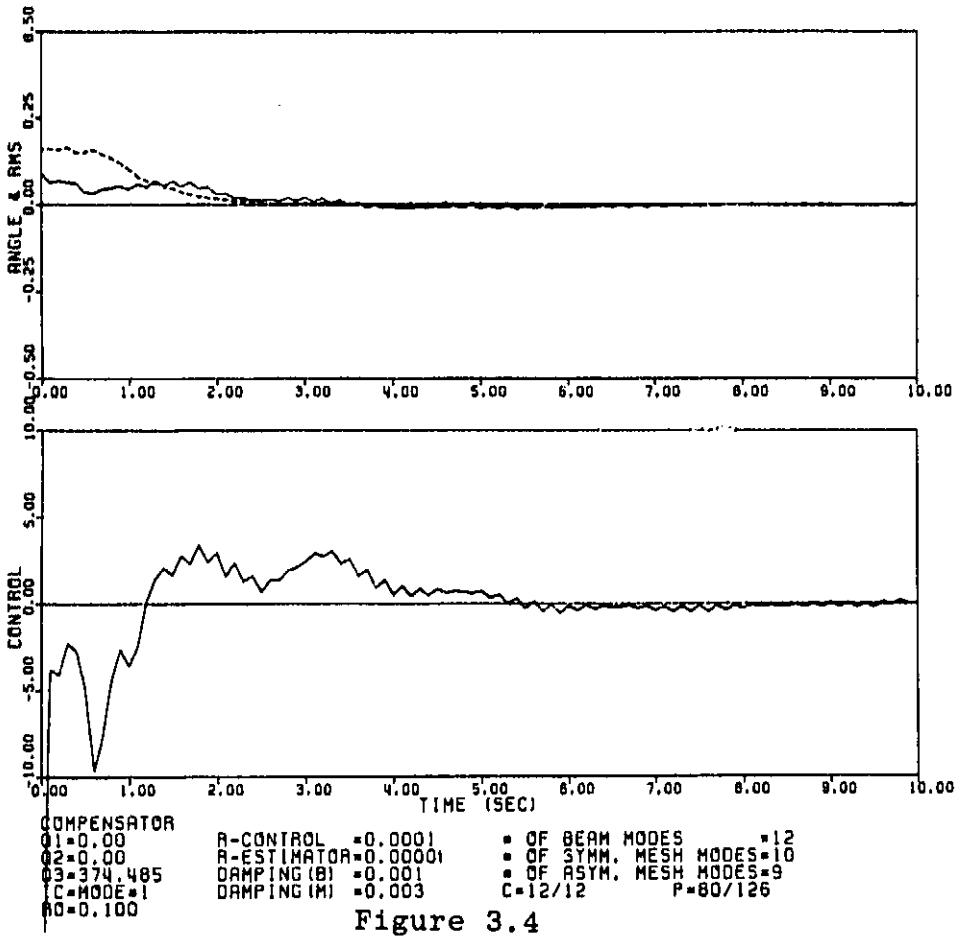

COMPENSATOR
Q1=0.00
Q2=0.00
Q3=374.485
IC=MODE=1
R0=0.100

R-CONTROL =0.0001
R-ESTIMATOR=0.00001
DAMPING(B) =0.001
DAMPING(M) =0.003

# OF BEAM MODES =12
# OF SYMM. MESH MODES=10
# OF ASYM. MESH MODES=9
C=12/12 P=80/126

Figure 3.4

ρ =.1 is noticeably more oscillatory than that for ρ = .01. The onset of oscillatory behavior is frequently a precursor of instability. Figures 3.5 - 3.7 are similar graphs for N = 8. Again, the oscillatory behavior seems to give advance warning of impending instability. In Figures 3.8 - 3.11, ρ is .1 and 1.0, and N is 16 and 22. The time histories for corresponding values of ρ are almost identical, as one might expect from looking at Figure 3.1. There is no evidence of oscillatory behavior.

An observation worth making with respect to these figures is that instability seems to develop rather quickly as ρ is increased. This emphasizes the importance of having an approach which insures that the model used for compensator design is a "good one."

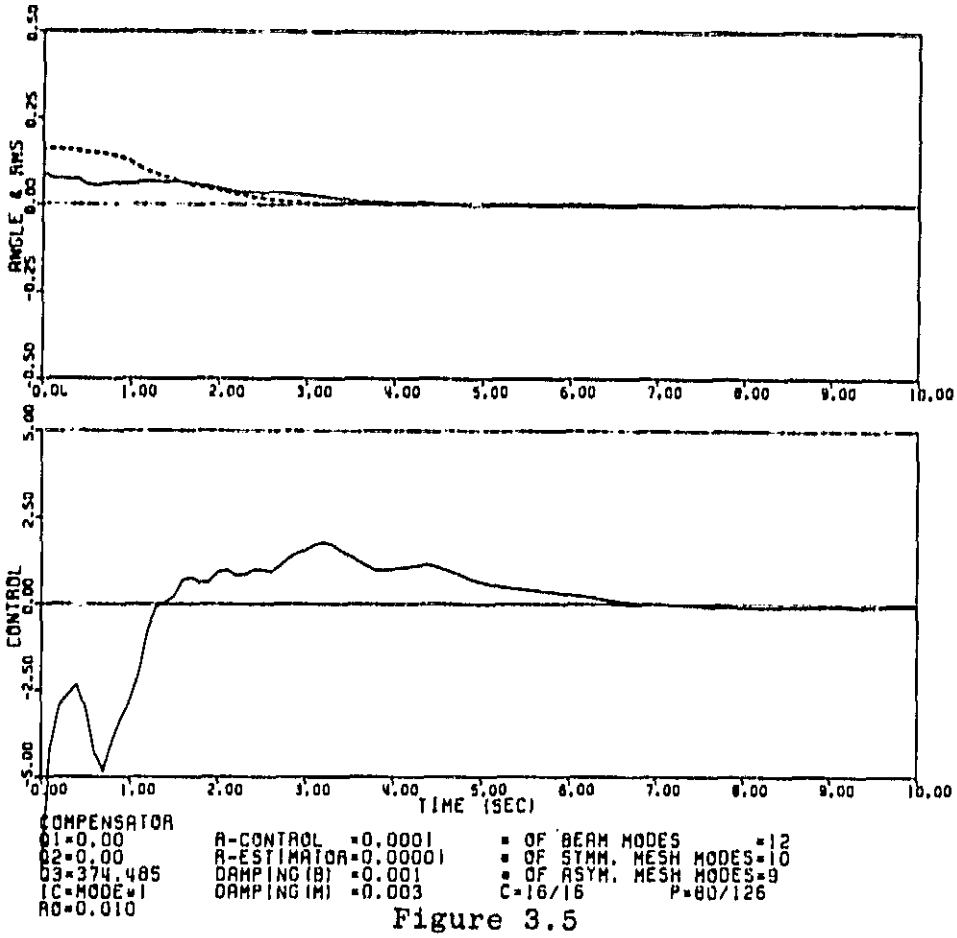

Figure 3.5

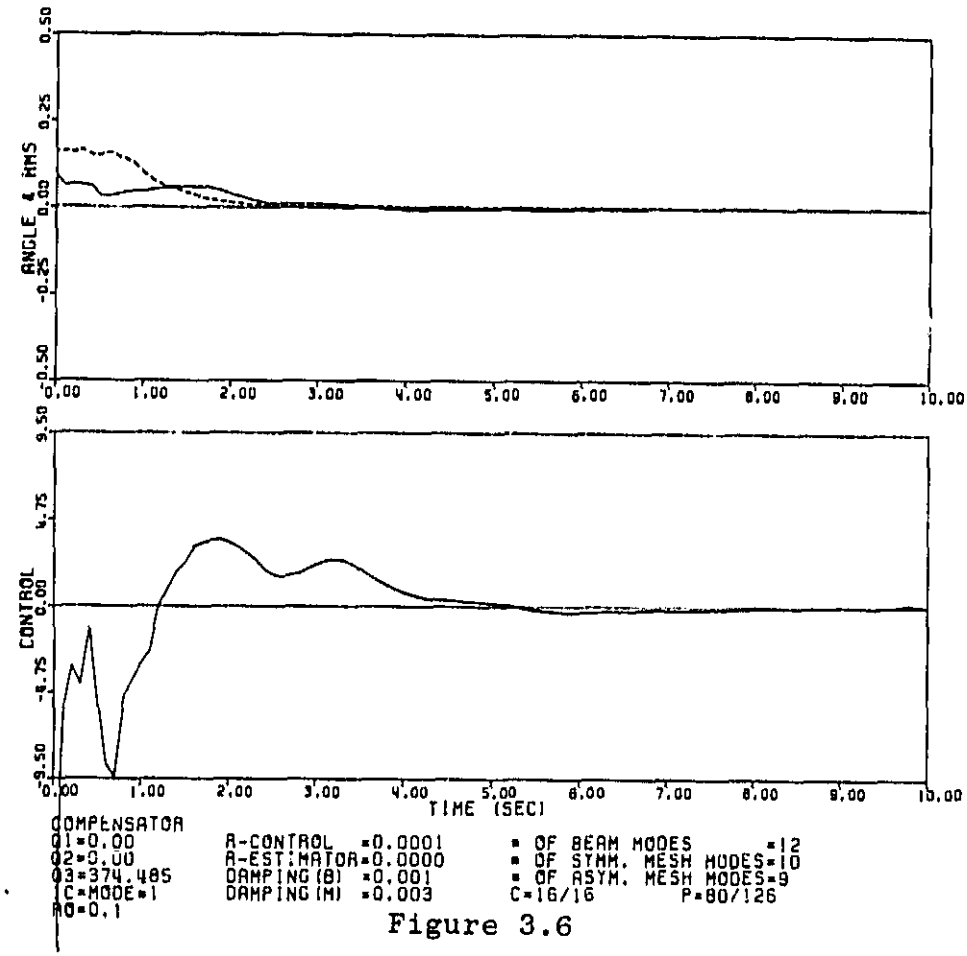

Figure 3.6

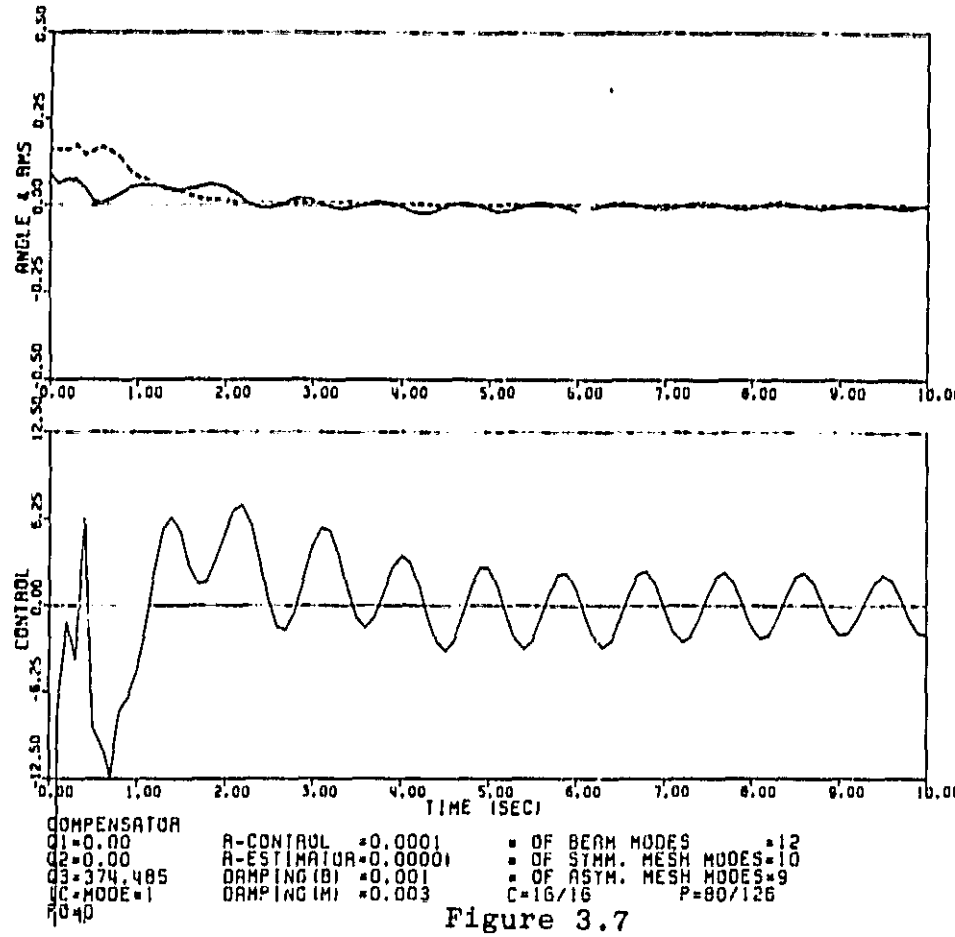

Figure 3.7

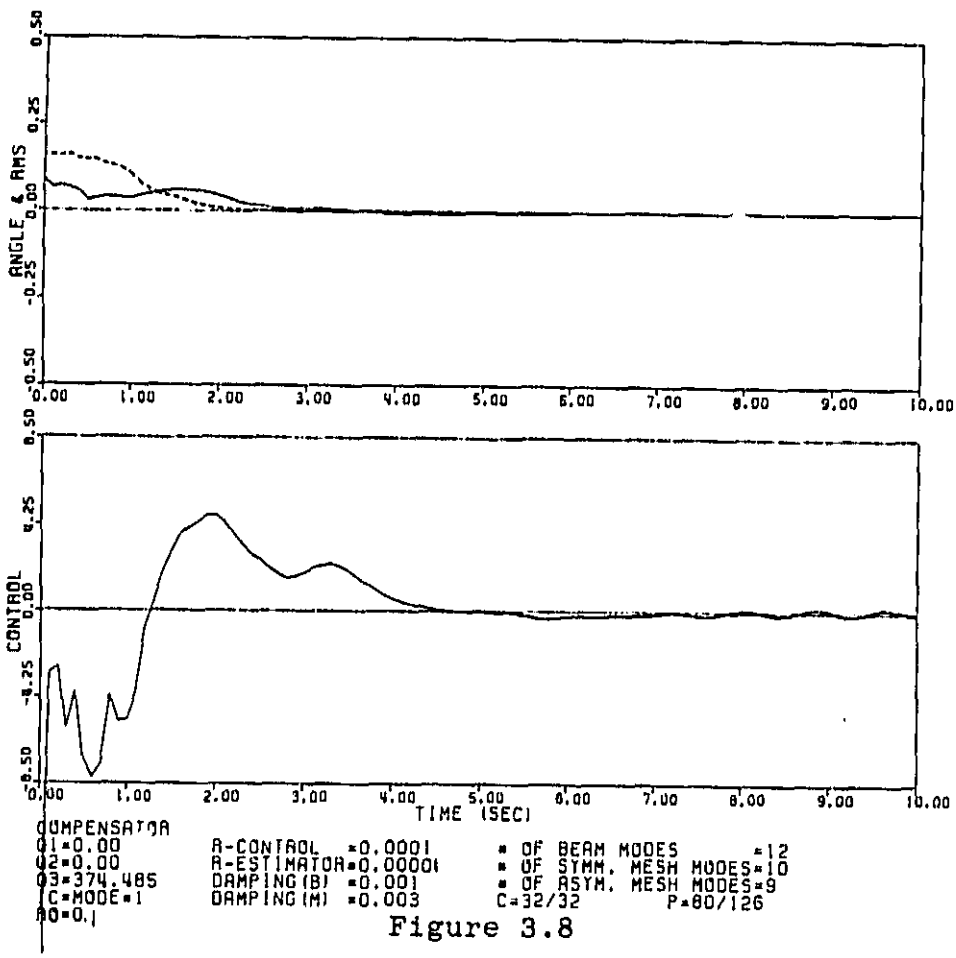

Figure 3.8

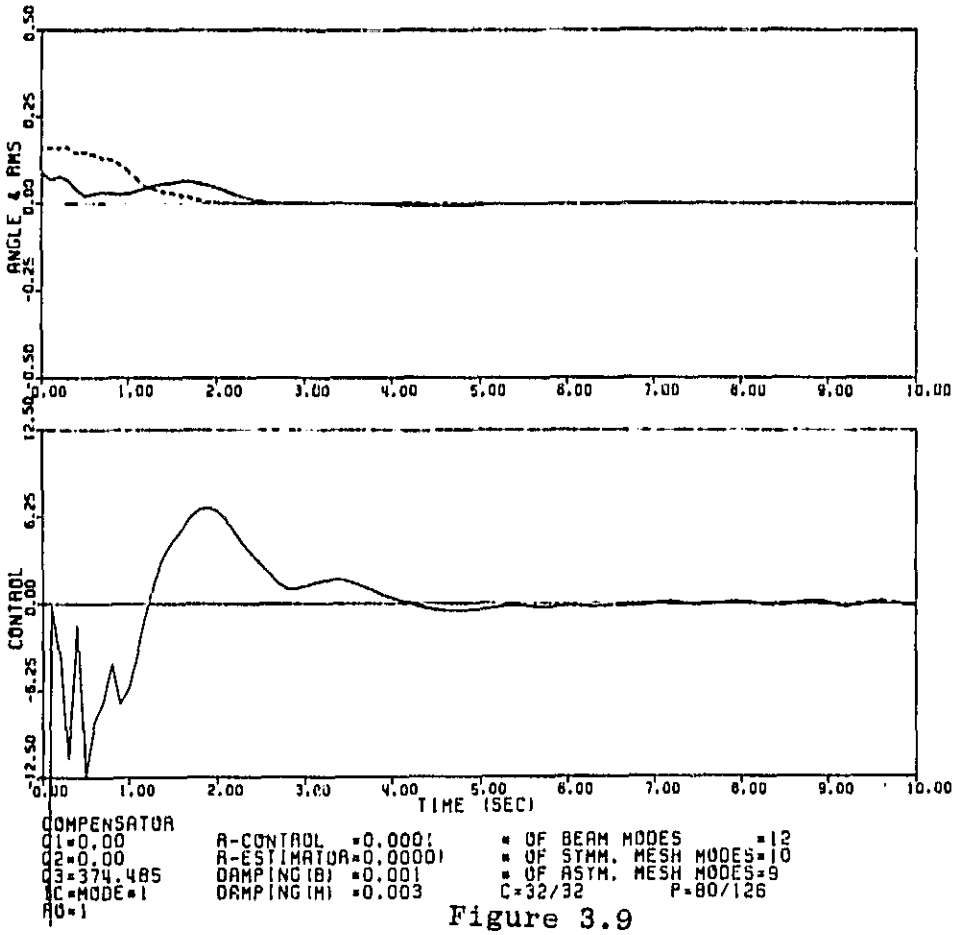

COMPENSATOR
Q1=0.00
Q2=0.00
Q3=374.485
IC=MODE=1
R0=1

A-CONTROL =0.0001
A-ESTIMATOR=0.00001
DAMPING(B) =0.001
DAMPING(M) =0.003

# OF BEAM MODES =12
# OF STMM. MESH MODES=10
# OF ASTM. MESH MODES=9
C=32/32 P=80/126

Figure 3.9

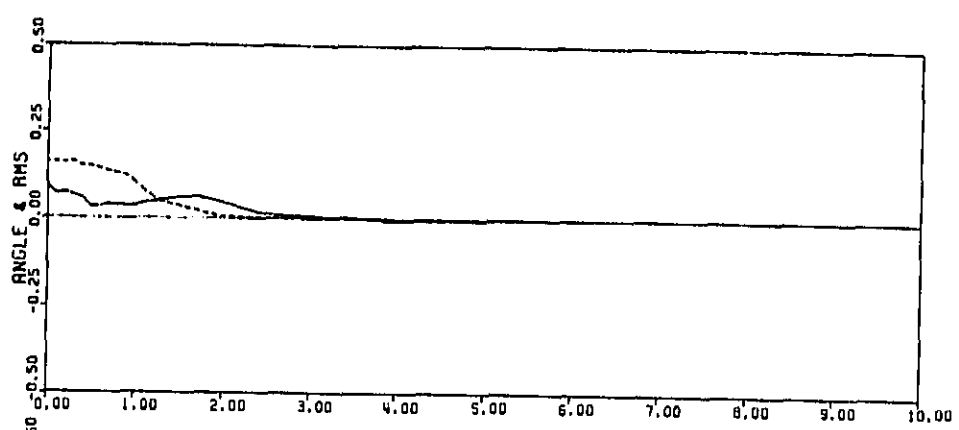

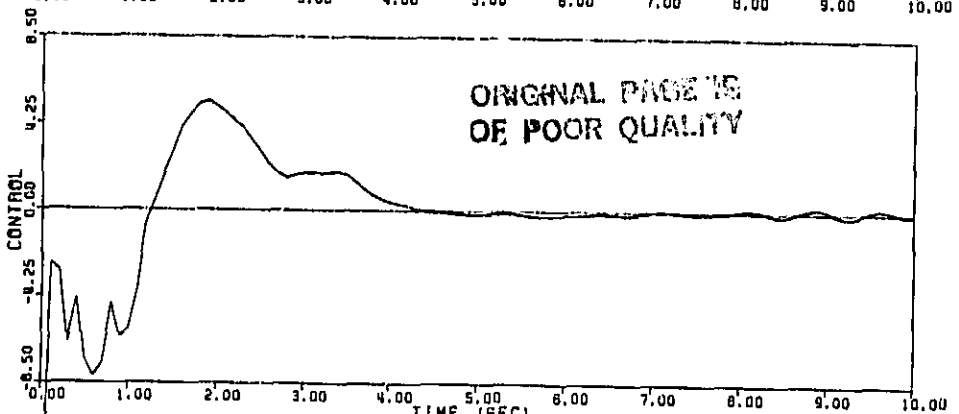

ORIGINAL PAGE IS
OF POOR QUALITY

COMPENSATOR
Q1=0.00
Q2=0.00
Q3=374.485
IC=MODE=1
R0=0.1

A-CONTROL =0.0001
A-ESTIMATOR=0.00001
DAMPING(B) =0.001
DAMPING(M) =0.003

# OF BEAM MODES =12
# OF STMM. MESH MODES=10
# OF ASTM. MESH MODES=9
C=44/44 P=80/126

Figure 3.10

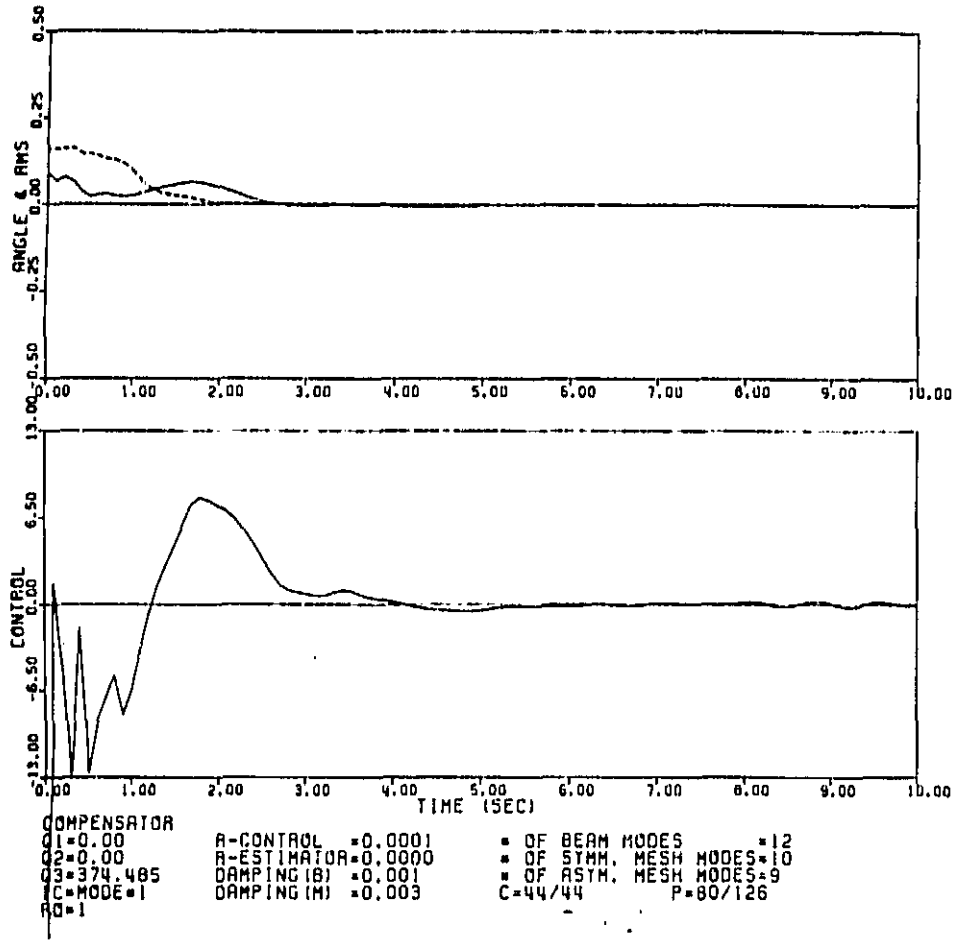
ANGLE & RMS
0.50
0.25
0.00
-0.25
-0.50
0.00
1.00
2.00
3.00
4.00
5.00
6.00
7.00
8.00
9.00
10.00
CONTROL
13.00
6.50
0.00
-6.50
-13.00
TIME (SEC)
COMPENSATOR
Q1=0.00
Q2=0.00
Q3=374.485
MC=MODE=1
R0=1
R-CONTROL =0.0001
R-ESTIMATOR=0.0000
DAMPING(B) =0.001
DAMPING(M) =0.003
# OF BEAM MODES =12
# OF STRM. MESH MODES=10
# OF ASTM. MESH MODES=9
C=44/44
P=80/126

Figure 3.11

IV. ROBUSTNESS

Robustness of the compensators is checked by performing simulations.

A 63-mode model is chosen as the evaluation model. Compensators based on 8 and 22 modes are chosen as representative compensator models. The scalar weighting factor ρ is chosen to be 1.

First, the simulations are performed with the nominal mass and stiffness matrices. Figures 4.1 and 4.2 show the control torque when the initial orientation error of the rigid body is 5 degrees and the system is brought to rest minimizing the surface error. System and sensor noise are not considered in the simulation.

For the other set of simulations, a random modal matrix and random frequencies are used. Appendix A shows how the random modal matrices and the random frequencies are generated.

Two cases are considered here. In the first case the random mode shapes vary at most 5% from the nominal mode shapes. In the second case the variations in the random mode shapes from the nominal mode shape increase as the mode numbers increase. For example the ith random mode varies at most (i + 3) percent from the nominal. The second case is supposed to represent the known observation that mode shapes with higher mode numbers have higher uncertainty.

For each case two different realizations are obtained. Eigenvalues of the closed loop system are obtained to ascertain the stability. In the first case, where uncertainty is uniform in all modes, the closed loop system with the compensator based

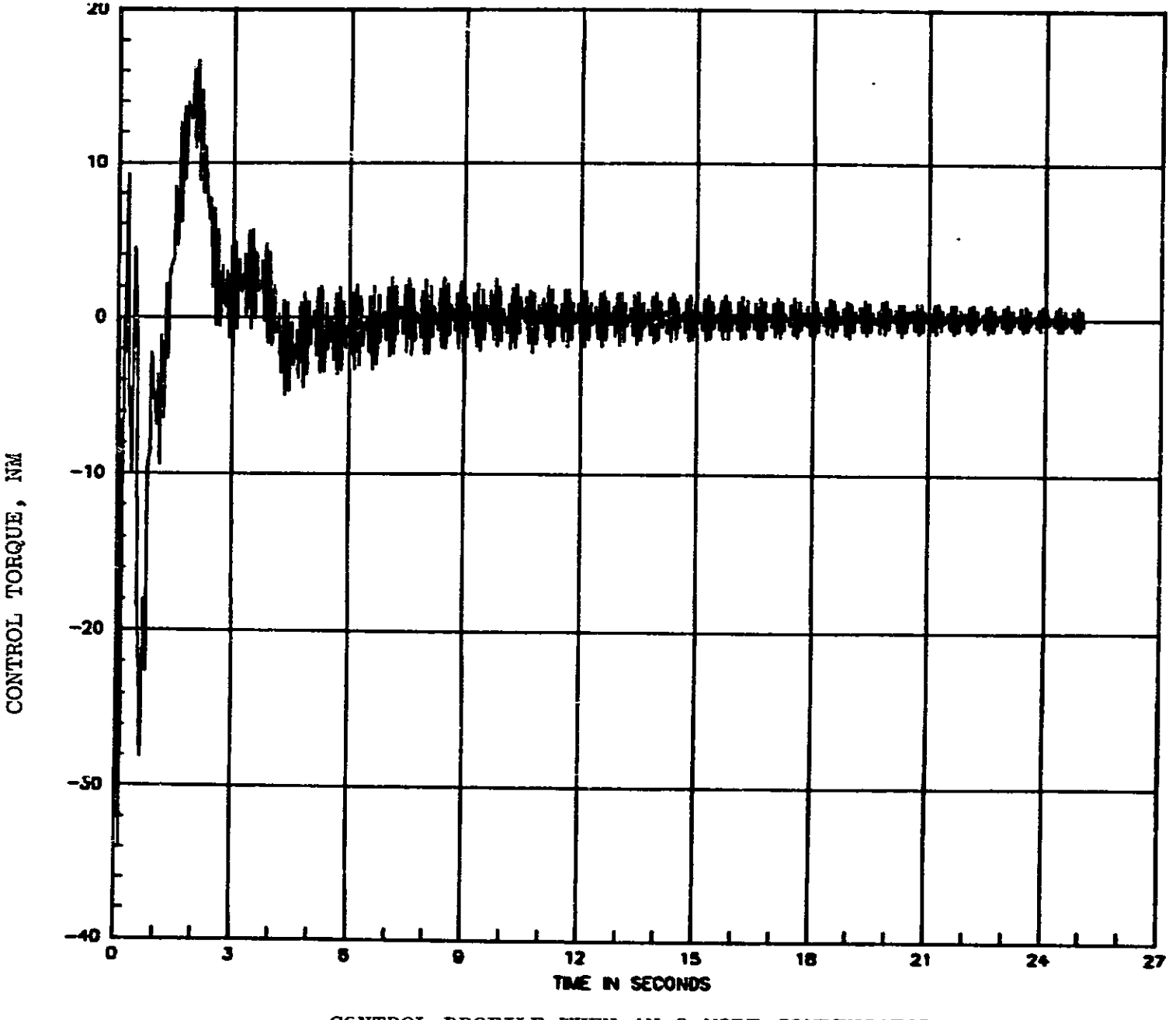

CONTROL PROFILE WHEN AN 8-MODE COMPENSATOR
IS APPLIED TO THE NOMINAL PLANT

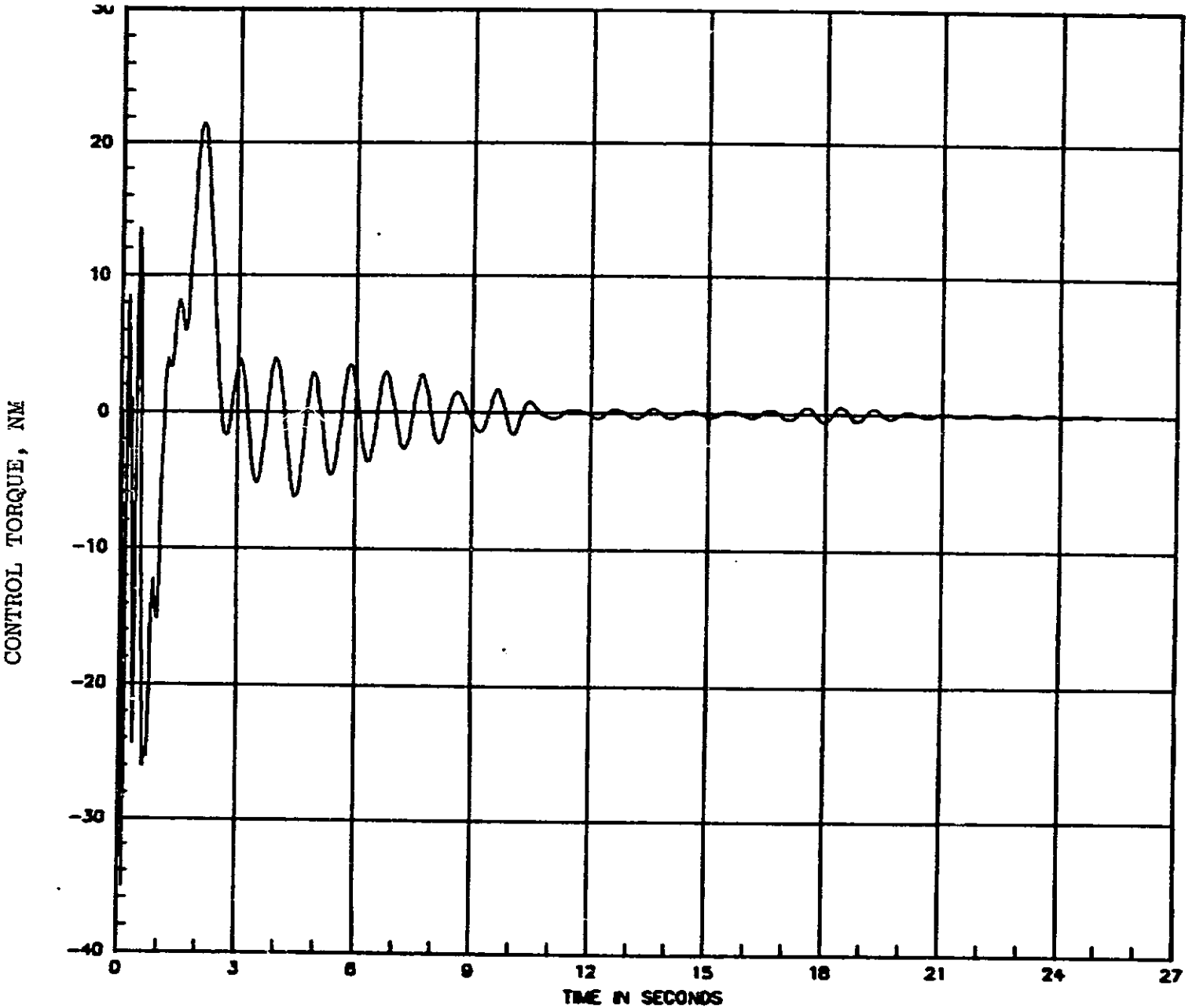

CONTROL PROFILE WHEN A 22-MODE COMPENSATOR
IS APPLIED TO THE NOMINAL PLANT

HR TEXTRON

Figure 4.2

on 22 modes is found to be stable for both the realizations. The closed loop system with the compensator based on 8 modes is found to be stable for one realization and unstable for the other realization. In the second case, where uncertainty increases with the mode numbers the closed loop system with the compensator based on 22 modes is found to be unstable for both the realizations. The closed loop system with the compensator based on 8 modes is found to be stable for one realization while unstable for the other realization. The results do not particularly show any trend, i.e., the closed loop system with the compensator based on high fidelity model is more stable. It is cautioned here that the following remark is based on a small sample. The compensators developed in this research project are based on LQG design which is a performance oriented design rather than a robustness oriented design. This clealy shows the need for more analytical and numerical simulation studies in the area of robustness for this research project.

IV.1 CONCLUSION

For the nominal system it is fairly obvious that the performance is better for the higher order compensator, as concluded in Section III.

In the case of randomly generated systems, generalizations are difficult to make. More analytical studies are needed.

One possible approach to stabilize the closed loop system is as follows. Obtain a compensator based on the techniques developed in this report for the nominal values of the

parameter. Use adaptive control techniques to fine tune this compensator for the particular system. This way the new compensator will be able to stabilize the closed loop system and hopefully be close to the optimal compensator for this particular system.

V. CONCLUSIONS

The results of this research project have shown that, for the distributed model of a flexible structure, an ideal compensator exists which can guide the design of implementable finite dimensional compensators. Also, the necessary order of a satisfactory implementable compensator depends on both the performance requirements and system characteristics, especially structural damping. The project has combined elements of optimal control theory for distributed systems to produce methods for designing implementable compensators for flexible space structures. These compensators approximate the ideal compensator.

An important feature of the methods developed is that the approximation theory associated with distributed-system control theory provides a framework and guidelines for automatically selecting a model of appropriate dimension on which to base the implementable compensator. Among the most promising tools to emerge are functional gains, modal gain energies and balanced states for distributed systems. All of these have served as primary indicators in the convergence analysis which determines the order of the near-optimal finite dimensional compensators.

VI. RECOMMENDATIONS

1) Further research is needed to develop the approximation guidelines of this project more fully and to develop algorithms for automatic computer implementation of these guidelines. Such research appears essential for computer-aided design of control systems for large flexible space structures.

2) In the work to date, the modeling was based on a finite element approach in which nodes and basis functions were selected to provide accurate descriptions of the natural modes and frequencies. Considerable study and experimentation was performed to identify nodes and basis functions which would perform this task efficiently. However, no attempt was made to have the control objectives, the control hardware, or location influence the model at the level of the finite elements. Control theory for distributed systems and the associated approximation theory should be used to develop methods, based on control system performance requirements, for optimal selection of finite element models. In this context, an optimal finite element model would be one of minimal order which provides the information necessary to design a compensator that produces the desired closed-loop performance. Such methods should be very useful for computer-aided design of control systems for flexible space structures.

3) Further investigation is required towards the robustness of the closed loop system. The following two techniques are suggested:

a. Frequency shaped performance criteria to reduce the sensitivity to errors in high frequency modes, and

b. System identification and adaptive control.

4) Practical uses of functional control and estimator gains, e.g., functional control gains possibly can guide sensor placements. Also, techniques are needed to develop functional gains from NASTRAN data.

5) The application of Balanced Realizations to distributed systems should be investigated. As discussed near the end of Chapter 5, Ref. [1] distributed models of flexible structures have balanced coordinates. Further development of the theory for these should enhance the application of Balanced Realization to large space structures.

6) The generation of realistic random plant models is needed to check the robustness of compensators using numerical simulations.

7) Adaptive control tecniques should fine tune the compensator based on the nominal plant values to ensure stability when the compensator is applied to a realistic (random) system. Theoretical studies need to be pursued in this direction.

REFERENCES

[1] HR Textron Report "Integrated Control/Structure Research for Large Space Structures", Final, September, 1984.

[2] "Space Technology, Lockheed Tests Large Space Antenna" Aviation Week and Space Technology, April 30, 1984.

[3] M.L. El-raheb, and P. Wagner "Static and Dynamic Characteristics of Large Deployable Reflector" Paper No. 81-0503-pc., presented at AIAA Specialists Conference in Atlanta, GA., April 1981.

APPENDIX A

A methodology to generate the random modal matricies and the random frequencies used in the robustness studies is presented here.

The random frequencies are obtained as follow:

$$w^r_i = w^n_i \ (1+.05 \ r_i) \quad i = 1, \ldots, 63 \qquad (A.1)$$

w^r_i is the i-th random frequency. w^n_i is the nominal i-th frequency. r_i is the gaussian random number with zero mean and unit variance. The magnitude of r_i is constrained in the following way to prevent extreme variations:

$$r_i = r_i \qquad \text{if } |r_i| \leq 1 \qquad (A.2)$$

$$r_i = r_i / |r_i| \qquad \text{if } |r_i| > 1 \qquad (A.3)$$

Thus, the random frequency varies at most 5% from the nominal value. The random modal matrix is generated in the following way:

$$V^r_{ij} = V^n_{ij} \ (1 + \sigma_j \ r_{ij}) \qquad (A.4)$$

V^n_{ij} is the i-th component of the j-th mode of the nominal plant. r_{ij} is a gaussian random number with zero mean and unit variance generated by the computer. To avoid extreme variations, the following restrictions are put on r_{ij}:

$$r_{ij} = r_{ij} / |r_{ij}| \qquad \text{if } |r_{ij}| \geq 1 \qquad (A.5)$$

$$r_{ij} = r_{ij} \qquad \text{if } |r_{ij}| < 1 \qquad (A.6)$$

σ_j controls the variance of V^r_{ij}. Two distinct cases were generated. In the first case

$$\sigma_j = 0 \qquad \text{if } j = 1$$

$$\sigma_j = .05 \quad \text{if } j = 2, 3, \ldots, 63 \qquad (A.7)$$

That is the rigid body of the random modal matrix is the same as the nominal rigid body mode while the rest vary at the most 5%.

In the second case

$$\sigma_j = 0 \qquad \text{if } j = 0$$

$$\sigma_j = .03 + j \quad \text{if } j = 2,3, \ldots, 63 \qquad (A.8)$$

In the second case, the rigid body mode is unchanged, but other modes have higher uncertainties as the mode number increases. For example, the second mode varies at most 5% from the nominal mode, while the 63-rd mode varies at most 66%.